GEOPHYSICAL RESEARCH LETTERS, VOL. 23, NO. 13, PAGES 1589-1592, JUNE 15, 1996

Finite fault source study of the great 1994 deep Bolivia earthquake

M. Antolik, D. Dreger, and B. Romanowicz

Seismographic Station, University of California, Berkeley, CA 94720

Abstract. We apply an empirical Green's function method to recordings of teleseismic body waves from the June 9, 1994 deep-focus Bolivia earthquake. The far-field source time functions reveal that rupture occurred on a sub-horizontal fault plane. The main rupture began some 25 km to the east of the hypocenter, consists of three large subevents, and covers a total area of about 60 x 40 km^2. The static stress drop is quite large, more than 150 MPa, and the obtained rupture velocity is less than 2 km/sec. While the total dimensions of the earthquake are large compared to estimates of the width of a metastable olivine wedge at this depth, the moment release is confined largely to a narrow band along an EW axis, and may be compatible with phase transitions within a thickened slab core.

Introduction

The recent large Bolivia earthquake (9 June, 1994; M_w 8.3; depth 637 km (NEIC)) represents the best opportunity to date to test the validity of mechanisms which have been put forth to explain the occurrence of shear faulting at depths where brittle failure should not normally occur. Historically, only one other deep earthquake has occurred with $M > 8.0$, the 31 July, 1970 Colombian event (M_w 8.2; depth 653 km). Studies of this event have led to an ambiguous picture as to the total area spanned by the rupture (e.g., *Furumoto*, 1977). The much greater quality of data available for the Bolivia earthquake makes it possible to constrain the source parameters and rupture area with a high degree of confidence and using a variety of methods (e.g., *Kikuchi and Kanamori*, 1994; *Beck et al.*, 1995).

The most favored explanation of deep earthquake occurrence involves the transformation of metastable olivine within a subducted slab to its denser spinel structure, which is delayed due to lower temperatures and involves shear failure promoted by nonhydrostatic stress conditions (*Kirby et al.*, 1991; *Burnley et al.*, 1991). However the limiting temperature for this process is thought to be around 600° C (e.g., *Wu et al.*, 1993), and existing thermal models of the subduction process predict a metastable olivine wedge of almost negligible thickness below 600 km (e.g., *Helfrich et al.*, 1989). This poses a problem for the occurrence of M_w 8+ events at these depths. As aftershocks do not generally provide reliable constraints on the rupture area of deep shocks (*Willeman and Frohlich*, 1987), finite fault models are essential for this purpose. This study aims to derive such a model for the Bolivia event through the use of an empirical Green's function (EGF) technique applied to data from the USGS/IRIS and GEOSCOPE broadband seismograph networks.

Paper number 96GL00968
0094-8534/96/96GL-00968$05.00

Data Analysis and Method

The 1994 Bolivia earthquake occurred in a portion of the Nazca subduction zone with a pronounced kink in the slab strike, and where a previous gap in deep seismicity existed (Fig. 1). The focal mechanism (Harvard CMT) indicates a normal faulting event involving rupture on either an eastward striking vertical plane or sub-horizontal plane. Activity began with a M_w 7.0 event on 10 Jan. 94 located about 200 km to the west of the future main event and with a similar focal mechanism (Fig. 1). We selected this event as an EGF. Various body wave phases including direct P, pP, PP, and PKP were windowed and deconvolved from the mainshock using a frequency domain water-level method. The deconvolutions were performed on the vertical component seismograms at each station. Resulting estimates of the source time function (STF) of the mainshock (e.g., Fig. 4) show that moment release began slowly with a relatively small precursory event lasting for $\sim$ 10 sec. The main rupture contains three dominant subevents with a duration of $\sim$ 30 sec. The total duration of rupture is thus extremely short for such a large event. The STFs are estimates of the actual source time function relative to that of the EGF,and although the source duration of the EGF is short ($\sim$ 6 sec), slight underestimation of the STF durations may result. However it was necessary to use the Jan. 10 event to achieve adequate signal power at epicentral distances greater than 30°. Some representative waveforms are shown in Fig. 2.

The STFs were used to obtain a map of moment release and estimates of the source parameters for the June 9 event by using a finite fault inversion technique introduced by *Mori and Hartzell* (1990) at local distances. This method maps the STFs onto the spatial and temporal slip distribution by allowing directivity in any direction while confining the rupture to one of the nodal planes. Following Dreger (1994) we solve a system of equations relating the observed STF at each station to the time function and slip amplitude of each subfault on the grid according to least squares with slip positivity and spatial derivative smoothing constraints. The inversion assumes a radially expanding rupture front with constant rupture velocity and dislocation rise time. The subfault time functions are assumed to be boxcars. The travel time for each phase is calculated from the global iasp91 velocity model. Actual values of slip are

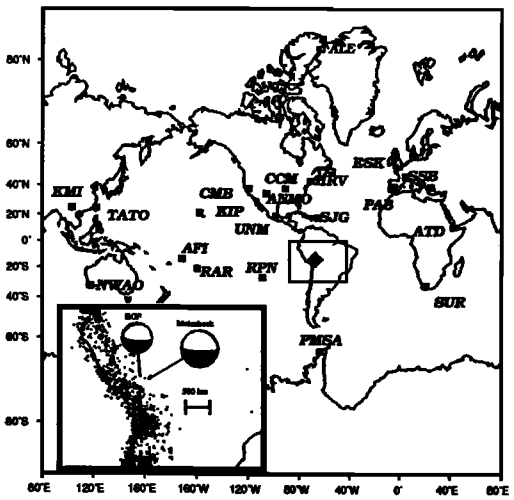

Figure 1. Map of the region of the great June 9, 1994 deep Bolivia earthquake (inset) and the global distribution of stations used in the present study. Inset shows focal mechanisms (Harvard) of the mainshock and the smaller event used as an emprical Green's function (see text) along with a 5-year sample of background seismicity. Epicentral data is from the NEIC.

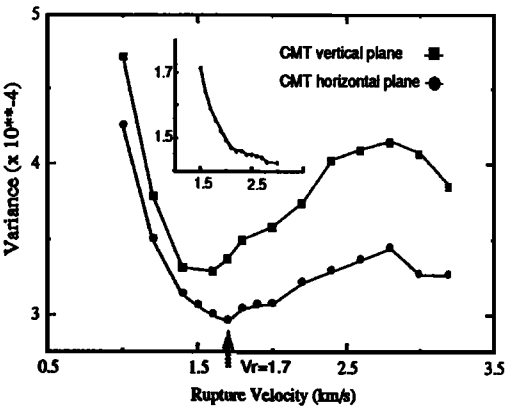

Figure 3. Plot of variance vs. rupture velocity for inversions of STFs. A horizontal fault plane gives a consisently better solution, and a minimum occurs at a value of 1.7 km/s (arrow). Variance is defined as the ratio of squared data misfit to the number of degrees of freedom. Inset shows the result of inversion of only the main portion of the STFs for the horizontal plane. There is no longer a minimum solution, but there is indication that the rupture velocity may have increased slightly during the main rupture phase.

obtained by using the moment value from the Harvard CMT solution ($3.0 \times 10^{21} Nm$) and represent average values over the area covered by each subfault. The total grid size is 180 x 180 km^2 and divided into subfaults with an area of 25 km^2.

Results

Prior to inversion, the STFs were low-pass filtered at 10 sec period to remove high frequency noise. We inverted a set of 20 STFs consisting primarily of direct P-waves but including a number of other phases. Each time function is assumed to represent the complete slip history and is normalized to unit area over the entire data set. For each nodal plane, the rupture velocity was varied from 1.0 to 3.4 km/s and the rise time from 2.5-7.5 sec. The best fitting solution is chosen to minimize a variance function defined as the ratio of squared misfit between data and synthetics to number of degrees of freedom in the model, which varies according to the number of subfaults having non-zero slip (*Mori and Hartzell*, 1990). The number of free parameters in the solution is important in assessing the validity of the model, as it is usually possible to fit the data better at unrealistically high rupture velocities as the rupture dimension increases.

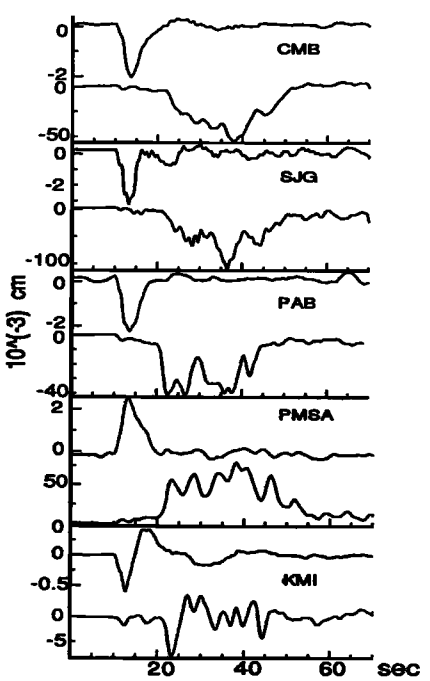

Figure 2. Vertical component displacement records (low-pass filtered at 1 Hz) for the Jan 10 EGF and the Jun 9 mainshock, respectively, are shown at the top and bottom of each subplot for selected stations. The entire window used for the deconvolutions is shown.

For all values of rupture velocity tested, the horizontal nodal plane (strike 302°, dip 11°) gave a better fit to the data (Fig. 3). A minimum was obtained at a value of 1.7 km/s, although there is little variation between 1.4 and 2.0 km/s. The best dislocation rise time is 5 sec. An F-test applied to the variances indicates that the significance level of the improvement in fit afforded by the horizontal plane is 85% at the minimum, and we conclude that this plane represents the rupture plane. However, rupture of sub-parallel vertical planes would probably not be resolved by this method and such a scenario, though unlikely, should not be ruled out. The fit of synthetics to the data is shown in Fig. 4. Generally the STFs are fit well, although the phasing of subevents is off at a few stations. This indicates that the rupture is well explained by a radially expanding fault model along a single plane at low frequencies.

A number of features of the model were found to be well resolved (Fig. 5). The main rupture is offset about 25 km to the east of the hypocenter, from which it is separated by a patch of little or no slip. The three large subevents cover an area of about 60 x 40 km^2, and rupture bilaterally to the north and south. The onset of the main rupture is extremely abrupt. In addition,

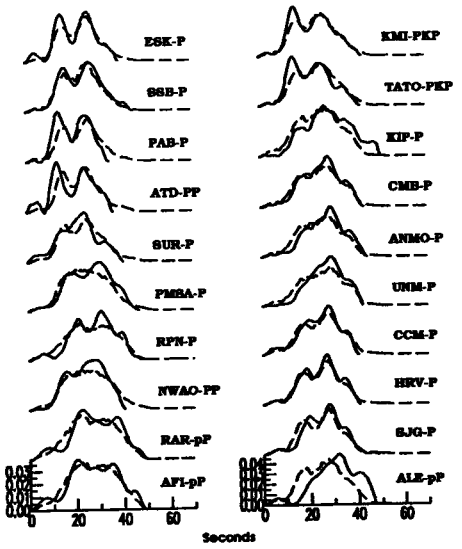

Figure 4. Data (solid) and synthetic STFs (dashed) for the best fitting fault model shown in Fig. 5. The observed STFs have been low-pass filtered at 10 sec. Amplitudes reflect normalization to unit area. The station and phase are indicated at right.

the initial precursory event consists of two resolvable subevents and ruptures primarily to the west, away from the area of large moment release. Although the majority of slip is concentrated along an EW axis, along

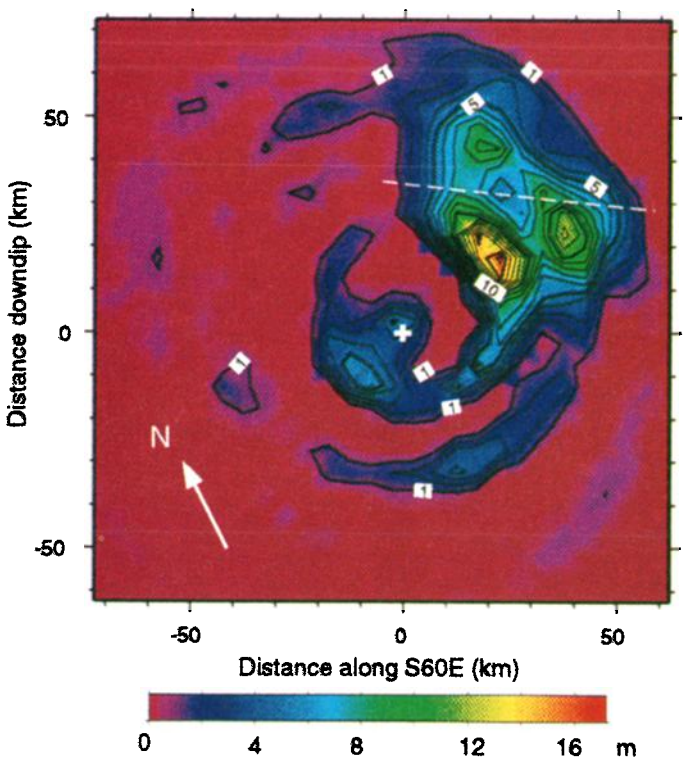

Figure 5. Slip map obtained from inversion along the horizontal plane with a rupture velocity of 1.7 km/s and dislocation rise time of 5 s. View is normal to the fault plane. The distribution shows the main rupture offset 25 km to the east of the hypocenter in a fan-shaped region. The peak value of slip is 16.5 m. Contour inverval is 1 m. The hypocenter is indicated by the cross and the dashed line indicates the strike of the aftershock distribution determined by *Myers et al.* (1995).

Table 1. Bolivia Earthquake Source Parameters

	Entire Rupture	Precursor	Main Rupture
Rupture velocity (km/s)	1.4-2.0	-	~ 2
Average slip (m)	4-6	2-4	-
Peak slip (m)	13-18	5-7	13-18
Rupture area (km^2)	4000-6000	~ 1700	-
Stress drop (MPa)	150-350	30-80	> 1000

the null axis of the focal mechanism, there is enough directivity in the NS direction to resolve a horizontal rupture plane. The small peak of slip at the south edge of the rupture is not robust and is greatly reduced in amplitude at lower rupture velocities. Also visible are arcuate patches of low level slip to the west (~ 3% of peak value). These represent artifacts of the radially expanding rupture and were ignored in calculating the source parameters.

The primary difference between these results and those of other published studies is the presence of the large subevent about 45 km to the east of the hypocenter. Although *Kikuchi and Kanamori* (1994) obtain a subevent located in this area, it is offset slightly to the north. *Silver et al.* (1995) give no indication of slip in this area, although one large pulse of moment release (E2) is ignored in their analysis. The overall dimensions of rupture are similar to those obtained by *Silver et al.* (1995). Their later subevents are located around the northern boundaries of the rupture shown in Fig. 5, which may indicate that they represent stopping phases. However since our inversion is only sensitive to long wavelength features we cannot rule out some minor slip patches in these areas. Some differences may also be caused by our constraint of a constant rupture velocity.

The average slip is 4-6 m, and we obtain a peak value of 16.5 m in the best fitting model. To calculate stress drop, we first estimate the rupture area by summing the areas of the subfaults with significant slip, then use equation (3) of *Kikuchi and Ishida* (1993). The small total rupture area for such a large shock leads to a stress drop in excess of 150 MPa. The local stress drop within the largest subevent exceeds 1 GPa. The initial event has a moment of 1.5-3 x 10^{20} Nm and a stress drop of 30-80 MPa. The calculated source parameters are summarized in Table 1.

We can resolve no slip in the gap between the hypocenter and the main rupture. This suggests that the rupture may have terminated and reinitiated with a higher velocity, perhaps involving a different mechanism. We examined this question by redoing the calculations after repicking the STFs at the onset of the main moment release. There is no longer a minimum in the variance (inset , Fig. 3) which becomes essentially constant above 2.0 km/s. Thus there is evidence that the rupture velocity may indeed have increased slightly during the event.

Discussion and Conclusion

It has been proposed (*Silver et al.*, 1995) that this event resulted from slip on a previously existing fault formed during a great normal faulting event when this portion of the slab was at a shallow depth. However others maintain that the metastable slab core can be deformed and thickened by resistance to penetration of

the lower mantle, particularly in the presence of a similar curvature in the slab strike (*Kirby et al.*, 1995). The concentration of the moment release along an EW axis 25 km wide, including that of the precursory event, may be consistent with this idea as it indicates that the rupture was strongly temperature controlled. We suggest that this axis defines the strike of the slab. This strike differs by about 35° from the strike of the aftershock distribution (*Myers et al.*, 1995; Fig. 5); however the slip distribution shows curvature in the direction of moment release with the portion to the east of the hypocenter exhibiting a strike that is more consistent with the aftershocks. As pointed out by *Myers et al.* (1995), the location of the January 10 event is consistent with a slab which is bent toward the west. The gap in slip suggests that the slab may not be continuous through this bend.

One intriguing recent observation regarding large, deep earthquakes is the predominately horizontal extent of moment release. In addition to the 1970 Colombian and Bolivian events, this has also been suggested for the March 9, 1994 deep earthquake near the Fiji Islands (*Antolik et al.*, 1995; *Lundgren and Giardini*, 1995). This may be indicative of an isobaric process controlling the rupture, although the stress redistribution can clearly induce aftershocks both above and below the main rupture. The total lateral extent of the rupture (> 35 km across the slab) extends completely across the aftershock zone. Thus a separate mechanism may be responsible for the continuation of rupture outside the slab core. One plausible factor, suggested by *Kikuchi and Kanamori* (1994), is the inducement of melting during the rupture process. The olivine-spinel phase transition is exothermic and larger events may produce sufficient heat to drive the rupture past the edge of the metastable wedge, as may the heat generation due to the faulting itself. On the other hand, *Ogawa* (1987) suggested that melting associated with shear instabilites might cause earthquakes within a slab at realistic strain rates without the occurrence of phase transitions. Instability is enhanced in his model by the presence of localized shear zones, and this may suggest a role for preexisting failure planes in generating deep earthquakes. Present data on deep earthquakes are insufficient to distinguish between these two possibilities.

Acknowledgements. The manuscript benefited from reviews by M. Kikuchi, C. Estabrook, and one anonymous reviewer. The authors also thank S. Kirby and T. Wallace for helpful discussions. This manuscript is Contribution No. 96-3 of the UC Berkeley Seismographic Station.

References

Antolik, M., D. Dreger, and B. Romanowicz, Rupture process of the March 9, 1994 deep Fiji Islands earthquake using an empirical Green's function method, submitted to *J. Geophys. Res.*, 1995.

Beck, S., P. Silver, T. Wallace, and D. James, Directivity analysis of the deep Bolivia earthquake of June 9, 1994, submitted to *Geophys. Res. Lett., 22,* 2257-2260, 1995.

Burnley, P. C., H. W. Green, and D. C. Prior, Faulting associated with the olivine to spinel transformation in Mg_2GeO_4 and its implication for deep-focus earthquakes, *J. Geophys. Res., 96,* 425-443, 1991.

Dreger, D. S., Empirical Green's function study of the January 17, 1994 Northridge, California earthquake, *Geophys. Res. Lett., 21,* 2633-2636, 1994.

Furumoto, M., Spacio-temporal history of the deep Colombia earthquake of 1970, *Phys. Earth Planet. Inter., 15,* 1-12, 1977.

Helfrich, G. R., S. Stein, and B. J. Wood, Subduction zone thermal structure and mineralogy and their relationship to seismic wave reflections and conversions at the slab/mantle interface, *J. Geophys. Res., 94,* 753-763, 1989.

Kikuchi, M., and M. Ishida, Source retrieval for deep local earthquakes with broadband records, *Bull. Seism. Soc. Am., 83,* 1855-1870, 1993.

Kikuchi, M. and H. Kanamori, The mechanism of the deep Bolivia earthquake of June 9, 1994, *Geophys. Res. Lett., 21,* 2341-2344, 1994.

Kirby, S. H., E. A. Okal, and E. R. Engdahl, The 9 June 94 Bolivian deep earthquake: An exceptional event in an extroardinary subduction zone, *Geophys. Res. Lett., 22,* 2233-2236, 1995.

Kirby, S. H., W. B. Durham, and L. A. Stern, Mantle phase changes and deep earthquake faulting in subducting lithosphere, *Science, 252,* 216-225, 1991.

Lundgren, P., and D. Giardini, The June 9 Bolivia and March 9 Fiji deep earthquakes of 1994: I. Source processes, *Geophys. Res. Lett., 22,* 2241-2244, 1995.

Mori, J., and S. Hartzell, Source Inversion of the 1988 Upland Earthquake: Determination of a Fault Plane for a Small Event, *Bull. Seism. Soc. Am., 80,* 507-518, 1990.

Myers, S. C., T. C. Wallace, S. L. Beck, P. G. Silver, G. Zandt, J. Vandecar, and E. Minaya, Implications of spatial and temporal development of the aftershock sequence for the M_w 8.3 June 9, 1994 deep Bolivian earthquake, *Geophys. Res. Lett., 22,* 2269-2272, 1995.

Ogawa, M., Shear instability in a viscoelastic material as the cause of deep focus earthquakes, *J. Geophys. Res., 92,* 13,801-13,810, 1987.

Silver, P.G., S. Beck, T. C. Wallace, C. Meade, S. Myers, D. E. James and R. Kuehnel, Rupture Characteristics of the Deep Bolivian Earthquake of 9 June 1994 and the Mechanism of Deep-Focus Earthquakes, *Science, 268,* 69-73, 1995.

Willemann, R. J. and C. Frohlich, Spatial patterns of aftershocks of deep focus earthquakes, *J. Geophys. Res., 92,* 13,927-13,943, 1987.

Wu, T. C., W. A. Bassett, P. C. Burnley, and M. S. Weathers, Shear-promoted phase transitions in Fe_2SiO_4 and Mg_2SiO_4 and the mechanism of deep earthquakes, *J. Geophys. Res., 98,* 19,767-19,776, 1993.

Received: August 8, 1995; Revised: February 1, 1996; Accepted: February 1, 1996